

# SURROGATE MODELLING FOR EFFICIENT DESIGN OPTIMIZATION OF COMPOSITE AIRCRAFT FUSELAGE PANELS

**W.J. Vankan\*, R. Maas\***

**\* National Aerospace Laboratory – NLR**

**Aerospace Vehicles Division**

**PO Box 90502, 1006 BM Amsterdam, the Netherlands**

**tel: 0031-20-5113059**

**fax: 0031-20-5113210**

**email: vankan@nlr.nl**

**Keywords:** *Multi-level optimization, BLISS, least-squares, mixture of experts*

## Abstract

*This paper considers a new methodology for large scale optimization that involves structural design analyses by finite element method (FEM) models of a composite aircraft fuselage barrel. A natural decomposition of the overall design optimization problem into two levels, i.e. the fuselage barrel level and the level of the individual fuselage panels, exists in these analyses. Therefore we implemented a variant of the multi-level optimization methodology known as BLISS (Bi-Level Integrated System Synthesis), which we first apply to a relatively simple test case based on the 10-bar truss optimization problem. In the fuselage barrel optimization, the decomposition into two levels allows for fast analysis with relatively coarse models of the whole fuselage barrel, while much more detailed models are used for the panel level analyses. These detailed panel models may include specific composite material properties like lay-ups and fiber orientations and detailed geometric aspects of frames and stringers. For further speed-up of the optimization process we apply surrogate modeling methods for the representation of the sub-system behavior. In this way the design variables that originate from the different model levels can be incorporated in a computationally efficient manner.*

## 1 Introduction

Ongoing developments in materials technologies have enabled the continuous improvement of airframe structures through the introduction of new materials and the related manufacturing processes. For example, composite materials allow for the design of more integrated and lighter structures that potentially require less maintenance than the traditional metallic ones. Composites are increasingly used on business jets, regional and commercial aircraft, representing for example up to 50% of the structural weight for the Airbus A350 XWB [1].

Due to their material properties, design options and the wide range of possible fiber reinforcements, composite materials offer a huge range of design variables, with a strong dependency on manufacturing [2]. Hence these composite materials provide much extended design freedom, but also additional complications like anisotropic behavior, to the design and development of new products when compared to more traditional materials. Consequently, one of the major challenges in the design of airframe structures is to find the best combination of in-service aircraft performance versus lifecycle cost within a design space of unprecedented size and complexity.

When considering the design challenge as an optimization problem for a large structural aircraft component, such as the aircraft fuselage, the number of design variables in this optimization problem (i.e. the dimensionality of the design space) and the number of possible constraints will become extremely large. One approach to deal with such a large scale design optimization problem is to decompose the overall problem into a number of smaller scale design optimization problems. These smaller scale problems typically consider a series of aspects or sub-systems in various levels of detail. Such an approach is commonly referred to as multi-level optimization (MLO) [3].

In this paper we present an implementation of a variant of the MLO method known as BLISS (Bi-level integrated system synthesis) [4]. We apply this MLO method to the design optimization of a composite aircraft fuselage barrel. The multi-level decomposition into two levels allows for fast analysis with relatively coarse models of the whole fuselage barrel, and much more detailed models for the panel level analyses. The design variables that originate from the different model levels can be incorporated in a computationally efficient manner.

## 2 MLO background

MLO requires a proper consistency in the decomposition of the considered overall design optimization problem. In the past decades, various methods such as simultaneous analysis and design (SAND), Concurrent Subspace Optimization (CSSO), Collaborative Optimization (CO), have been developed for the decomposition and multi-level optimization of complex systems [5]. These methods originate predominantly from the field of Multidisciplinary Design Optimization (MDO), where an intrinsic decomposition of the overall design problem is normally required due to the multiple specific disciplinary analyses that are applied. Another method originating from the MDO field is BLISS [4], for which a more recent formulation was given by Agte et al. in

2005 [6]. In this formulation the system to be optimized is non-hierarchically divided into sub-systems, i.e., each sub-system may directly interact with each of the other sub-systems. In this paper we will build upon the latter BLISS formulation. The advantage of this BLISS formulation over ‘single-level’ or ‘All-in-One’ (AiO) optimization is that it allows the sub-systems to be concurrently optimized.

The BLISS optimization method [6] was designed for optimization of non-hierarchic systems involving multidisciplinary analyses (as in MDO). We made some further developments to the method, aiming for application to structural optimization problems with a more hierarchic nature. Among others, we implemented more appropriate surrogate (approximation) models of the sub-systems, applying specific local sampling methods and specific least-squares fitting methods.

## 3 MLO test problem: 10-bar truss

To illustrate the functionality of the MLO method we first show an application to a variant of the well-known structural optimization test problem of the 10-bar truss system (fig. 1).

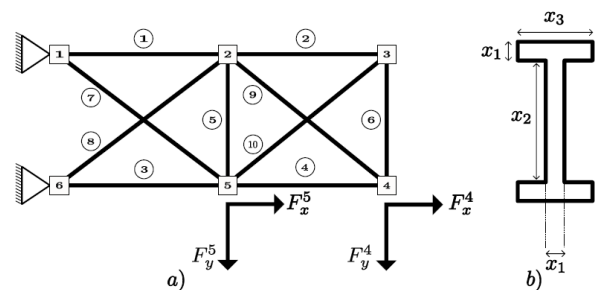


Fig. 1: The 10-bar truss system (left) and the cross-section of each bar with the design variables  $(x_1, x_2, x_3)$  of truss bar  $i$ .

The objective is to minimize the total mass of the system for given external forces  $(F_x^4, F_y^4, F_x^5, F_y^5)$ , subject to constraints related to maximum stress allowables and Euler buckling and local web buckling for the bars, using the design variables in the  $\mathbf{R}^3$  vector  $\mathbf{x}^{(i)} = (x_1, x_2, x_3)^{(i)}$  of each of the 10 truss bars as independent variables.

In an AiO optimization approach, the mass minimization of the whole system under the given constraints, is directly performed in the 30-dimensional space of the design variables of all 10 bars.

In a MLO approach the aim is to decompose the problem into separate and simplified optimizations on the level of the bar and on the level of the whole system. The advantage is that the bar optimizations are performed in the 3-dimensional space of the bar design variables. The disadvantage is that we need exchange of constraint information between the bar level and system level, which requires iterations of optimizations on the two levels.

For the problem decomposition in our MLO method we consider the cross-sectional area  $y^{(i)}=(x_1x_2+2x_1x_3)^{(i)}$  of each of the 10 bars as an additional set of independent variables, expressed by the  $\mathbf{R}^{10}$  vector  $\mathbf{y}$ . The mass of each bar depends only on the bar area  $y^{(i)}$  and not explicitly on the bar design variables  $\mathbf{x}^{(i)}$ . The forces in the bars ( $f^{(i)}$ ) in static equilibrium of the system under the external forces depend on the stiffness of each bar, which is proportional to the bar cross-sectional area  $y^{(i)}$ . Hence the allowable tension and compression stresses in each of the bars can be expressed as the stress constraints given in (eq. (5)) below. Two types of buckling constraints are considered in this problem: Euler buckling and local web buckling, expressed as:

$$f^{(i)} > -F_{Euler}^{(i)}; F_{Euler}^{(i)} = \frac{\pi^2 EI^{(i)}}{(L^{(i)})^2} \quad (1)$$

$$f^{(i)} > -F_{web}^{(i)}; F_{web}^{(i)} = \frac{4\pi^2 E}{12(1-\nu^2)} (R^{(i)})^2 \quad (2)$$

where  $L^{(i)}$  is the length,  $I^{(i)}$  is the second moment of area and  $R^{(i)}$  is the thickness-height ratio ( $x_1/x_2$ ) of bar  $i$  and  $E$  is Young's modulus  $\nu$  is Poisson's ratio of the (linear elastic) material of the bars. These buckling constraints depend on the bar forces ( $f^{(i)}$ ), but also have an explicit dependency on the bar design variables  $\mathbf{x}^{(i)}$  and are therefore expressed as given in (eq. (6)) below.

The 10-bar truss optimization problem can therefore be formulated as a system level minimization expressed in  $\mathbf{y}$  ( $\in \mathbf{R}^{10}$ ):

$$\min_{\mathbf{y}} M(\mathbf{y}) = \sum_{i=1}^{10} m^{(i)}(y^{(i)}) \quad (3)$$

subject to the constraints, expressed in  $\mathbf{x}^{(i)}$  ( $\in \mathbf{R}^3$ ) and  $\mathbf{y}$ :

$$c_{bound}^{(i)}(\mathbf{x}^{(i)}) \leq 0 \quad ; \quad \forall i \quad (4)$$

$$c_{stress}^{(i)}(f^{(i)}(\mathbf{y})) < 0 \quad ; \quad \forall i \quad (5)$$

$$c_{buckling}^{(i)}(\mathbf{x}^{(i)}, f^{(i)}(\mathbf{y})) < 0 \quad ; \quad \forall i \quad (6)$$

where  $m^{(i)}$  is the mass of truss bar  $i$  and  $M$  is the total mass of the system. The bounds on the bar design variables are explicitly expressed as a constraint function of  $\mathbf{x}^{(i)}$  (eq. (4)).

In our MLO method we now minimize on the bar-level the cross-sectional area ( $y^{(i)}$ ) of the bar under the given constraints (eqs. (4,5,6)) in the  $\mathbf{R}^3$  space of the bar design variables for a series of prescribed force values  $f^{(i)*}$ . This minimum bar area ( $y^{(i)}_{min}(f^{(i)*})$ ) is driven by the constraints: either the bound, stress or buckling constraint is active in the minimum, as illustrated in the figure (fig. 2) below. Obviously the buckling behavior of the long (diagonal) bars is slightly different from the short bars.

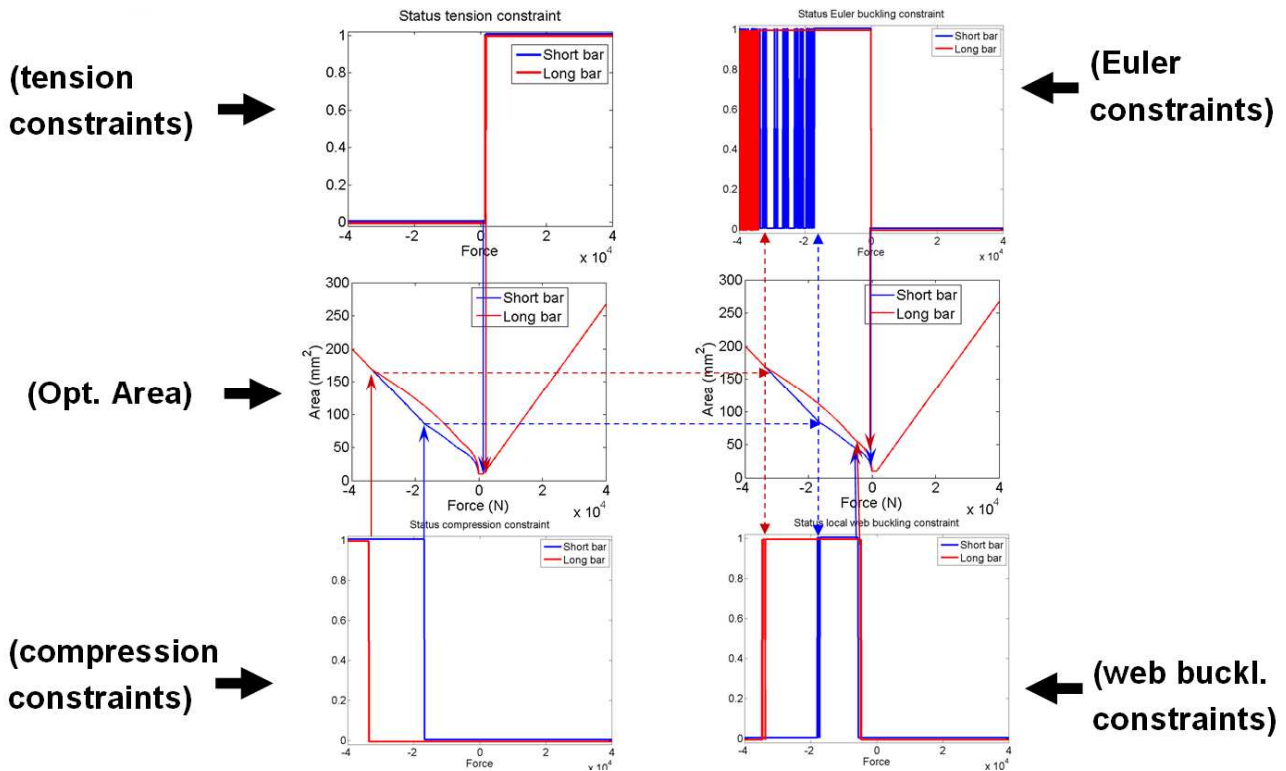


Fig. 2: The optimal cross-sectional areas (2 middle graphs) of the long (diagonal) bars (red curves) and short bars (blue curves) as a function of prescribed bar force ( $y_{\min}^{(i)}(f^{(i)*})$ ) for the bars in the 10-bar truss problem. These optimal bar areas depend on the various constraints that are active at each force value (as illustrated by the 2 upper and 2 lower graphs).

For very low tension force only the bound constraint is active (small horizontal part of the curves in the graphs), i.e., the minimum bar area is determined by the lower bounds of the bar design variables ( $x_1, x_2, x_3$ ). For higher tension force only the stress constraints are active. For low compressive force the Euler buckling constraints are active and for slightly higher compressive force also the web buckling constraints become active. For further increased compressive force the stress constraints become active, while the Euler constraint is nearly active (“switching on and off”). For the long bars (i.e., the diagonal bars in the 10-bar truss system, indicated by the red lines in the graphs) the buckling constraints remain active until higher compressive force values than for the short bars (i.e., the horizontal and vertical bars in the 10-bar truss system, indicated by the blue lines in the graphs).

From the bar level optimization results of minimum (allowable) bar area values as a function of prescribed bar force ( $y_{\min}^{(i)}(f^{(i)*})$ ), we

construct a surrogate model where the aim is to achieve optimal accuracy with as few as possible prescribed force sample points. Therefore we applied specific iterative local force sampling and various fitting methods to capture as good as possible the minimum (allowable) bar area (see fig. 3 below).

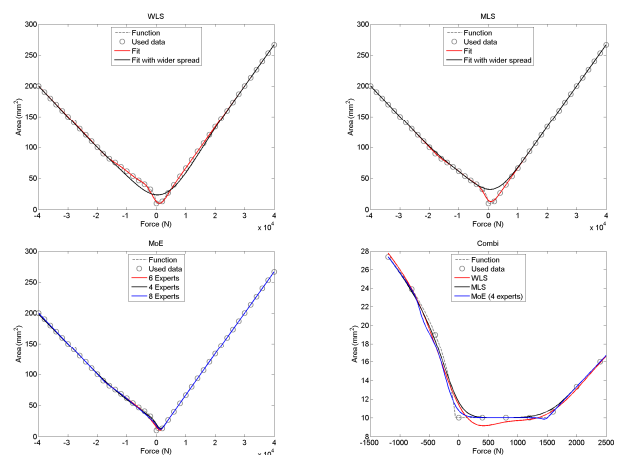


Fig. 3: Illustration of the surrogate model accuracy for minimum bar area as function of prescribed bar force obtained with various fitting methods: Weighted Least

Squares (WLS), Moving Least Squares (MLS) [9], Mixtures of Experts (MoE) [10], and the results for each of these fits for a specific local force sample in the central part of the curve.

The MoE method appeared to provide the most accurate surrogate model, and was applied with a local sampling in 6 force values per bar. The surrogate model of the minimum bar area as a function of bar force that has been determined on the bar level is subsequently used on the system level as an in-equality constraint function in the minimization of the total mass, where the force in each of the bars is determined from the system equilibrium ( $f^{(i)}(\mathbf{y})$ ):

$$y^{(i)} > y_{min}^{(i)}(f^{(i)}(\mathbf{y})) \quad (7)$$

A number of load-cases, using different external force vectors ( $F_x^4, F_y^4, F_x^5, F_y^5$ ), was evaluated with both the AiO and the MLO approaches. In comparison with the AiO optimizations, the MLO method yields similar values for the minimum total mass within 1% deviation from the AiO results. However, the computational efficiency, particularly in terms of function evaluations on the bar level, is lower for the MLO method; see table 1 below. But it should be noted that the bar evaluations involve only 2 dofs, whereas the system evaluations involve 8 dofs. All optimizations in the AiO and the MLO evaluations were run with the non-linear constrained minimization function (fmincon) of Matlab, where finite difference approximations of the gradients were used.

Table 1: Computational efficiency of the MLO method compared to the AiO optimization for one load-case of the 10 bar truss problem.

Method	Approximate nr. of Function evals. Sys. level / Subsys. level	Approximate nr. of Optim. iters. Sys.level / Subsys. level
AiO	400 / n.a.	12 / n.a.
MLO	200 / 5e3	20 / 1e3

## 4 Fuselage barrel MLO

The optimization of the fuselage barrel is aimed at minimization of the design objective, which is typically the fuselage weight. In analogy with the MLO method described above for the 10-bar truss problem, this is achieved through the two-level optimization approach in the following way. On the barrel level the optimization considers the minimization of the structural mass, taking into account constraint information coming from the panel level analyses. The loads on panel level are estimated by applying the fuselage loads (like axial compression, torsion, internal pressure, bending) to the coarse fuselage barrel model. The panel dimensions (like skin thickness, stringer height, fiber orientations) are then optimized on the panel level, subject to typical design constraints (such as buckling load, allowable mechanical stress, etc.) through evaluation of the detailed panel model.

In analogy with the high number of sub-system evaluations in the 10-bar truss problem (table 1), the panel level optimization process may require many evaluations of the detailed panel model, in particular if many design variables and constraints are considered on panel level. To overcome the computational burden and the process complexity of evaluating the detailed panel FEM model directly inside the optimization loop, computationally efficient surrogate models for the panel behavior are built and deployed. These surrogate models basically represent the values of the objective and constraint functions on panel level (such as panel weight, maximum stress, minimum buckling load factor) as a function of the panel design variables. They are built by applying various surrogate modeling methods [7] like least squares polynomial fitting, kriging models, neural networks and radial basis functions, to data sets of the panel behavior that are obtained from series of simulations with the detailed panel FEM model.

#### 4.1 Barrel-panel optimization problem

The multi-level barrel-panel optimization that we consider in this paper is limited to the minimization of the fuselage barrel weight, where only the skin thickness ( $t_{skin}$ ) is used as the design variable with bounds  $1 \text{ mm} < t_{skin} < 5 \text{ mm}$ , and only skin buckling is used as constraint. Because we only consider the skin thickness as design variable and the optimization objective (weight) is linearly dependent on this variable, we will, instead, directly use skin thickness as objective function. Also only one barrel level load-case is considered, consisting of an axial compression of 5.4 MN (400 N/mm compression load intensity) and torsion about the fuselage axis of 5.8 MNm (200 N/mm shear load intensity). See fig. 4 below.

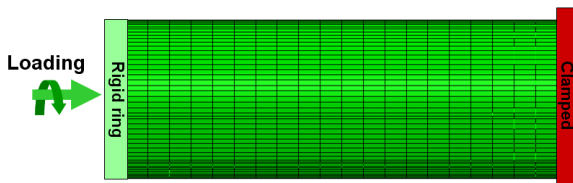


Fig. 4: Barrel loading considered in the multi-level barrel-panel optimization. Axial compression and torsion loads of 5.4 MN and 5.8 MNm, respectively, are applied via a “virtual rigid ring” attached to the barrel skin.

#### 4.2 Panel level analyses

The panel level analyses make use of a rather detailed parametric FEM model of a curved fuselage panel containing 5 stringers and 4 frames, which was implemented in the FEM software Abaqus version 6.9 [8]. The panel has a curvature radius of about 2150 mm, and approximately 200 mm stringer pitch and 650 mm frame pitch. Omega stringers of about 85 mm total width, 30 mm height and 2 mm thick, and C-frames of about 25 mm width, 85 mm height and 2 mm thick are used. The boundary conditions for this panel model suppress all rotations and radial displacements of all four edges. Furthermore the axial displacements are suppressed on one curved edge and equality-constrained on the other curved edge. The non-curved edges have linearly constrained

tangential displacements such that their angular rotation about the fuselage axis is linear over the full length of these edges. The panel model is loaded by a distributed axial compressive unit load (1 N/mm) on the equality-constrained curved edge, and by a distributed shear unit load on the straight edges (-1 N/mm) and on the curved edges (1 N/mm) (see fig. 5 below).

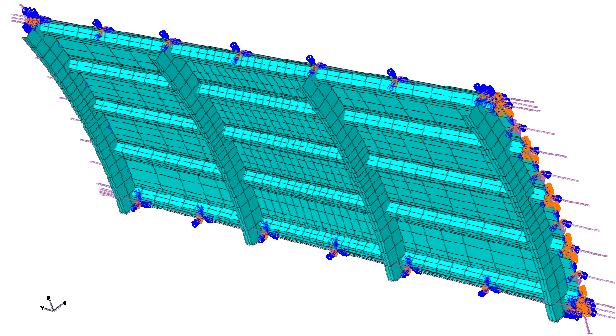


Fig. 5: FEM model of the curved panel with loading and boundary conditions. The clamped curved edge is on the left side.

The panel skin, as well as all the stringers and frames, are modeled by a total of approximately 3400 quadratic shell-elements (8 nodes, 48 dofs, S8R [8]), yielding about 11000 nodes and 42000 dofs for the whole panel model. Skin and stringers consist of a composite laminate with elastic ply properties given by the Young's and shear moduli and Poisson's ratio with approximate values:  $E_x=160\text{GPa}$ ,  $E_y=9\text{GPa}$ ,  $G=4\text{GPa}$ ,  $\nu=0.35$ . For the skin a fixed 8-ply stacking sequence ( $45^\circ/-45^\circ/90^\circ/0^\circ/0^\circ/90^\circ/-45^\circ/45^\circ$ ) is used with (25%, 25%, 25%, 25%) thickness contributions, respectively, for the ( $45^\circ/-45^\circ/90^\circ/0^\circ$ ) plies. As mentioned above, total skin thickness ( $t_{skin}$ ) is the design variable, which is varied between 1 mm and 5 mm. For the stringers also a composite with similar elastic properties as for the skin and a fixed 8-ply stacking sequence ( $45^\circ/-45^\circ/90^\circ/0^\circ/0^\circ/90^\circ/-45^\circ/45^\circ$ ) is used with (15%, 15%, 10%, 60%) thickness contributions, respectively, for the ( $45^\circ/-45^\circ/90^\circ/0^\circ$ ) plies. Aluminium frames are used with elastic material properties  $E=72\text{GPa}$ ,  $G=27\text{GPa}$ ,  $\nu=0.33$ .

The panel level analyses consider only linear buckling simulations, which were

evaluated using the Lanczos eigensolver [8]. Only the first 2 modes (see fig. 6 below) were evaluated requiring about 250 s CPU time on a standard PC (Pentium 4, 2.8 GHz).

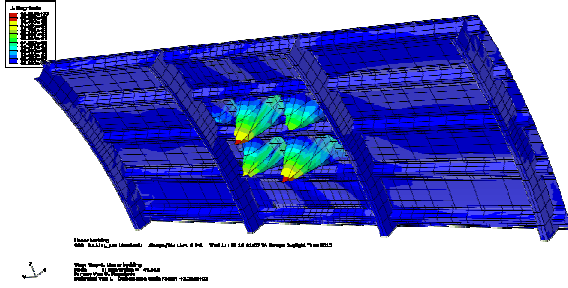


Fig. 6: Illustration of the first local buckling mode shape of the curved panel FEM model under combined compression and shear loading.

The panel buckling analyses described above were performed for a series of 5 skin thickness values, equi-distantly sampled between the lower and upper bounds (1mm and 5mm). In order to capture the panel buckling behaviour for various load conditions we also varied the ratio between compression and shear loading. This ratio is expressed by a compression-shear ratio angle ( $\varphi \in [0^\circ, 90^\circ]$ ), such that the compression loading  $l_c = \cos(\varphi)$  N/mm and the corresponding shear loading  $l_s = \sin(\varphi)$  N/mm. For proper sampling of these load combinations we selected 5 values for  $\varphi$  on approximately equi-angular positions in the loading plane (see fig. 7 below), resulting in a set of 5  $l_c$  values and corresponding  $l_s$  values.

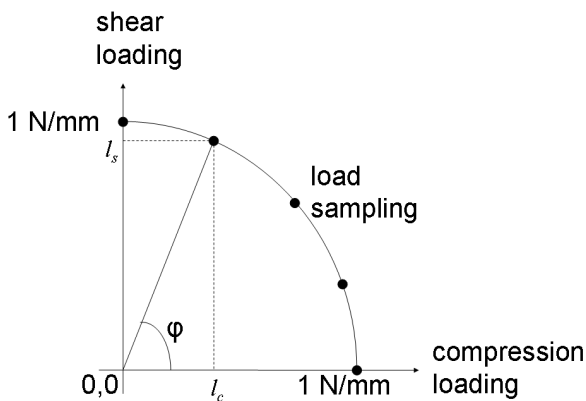


Fig. 7: Illustration of the considered compression and shear loading combinations in the panel analyses.

From the buckling evaluations for the 5x5 (full-factorial) sampling of skin thickness values and loading combinations, the eigenvalues

(buckling values,  $\lambda$ ) of the first mode were stored. The results are shown in the figure (see fig. 8 below).

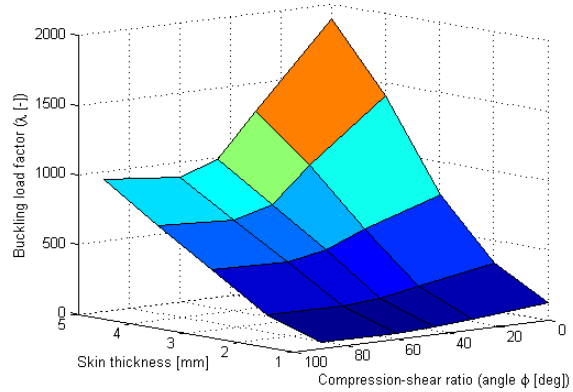


Fig. 8: Buckling values from the panel analyses, presented as a function of the skin thickness and compression and shear loading combinations.

To obtain an accurate surrogate model representation of the 5x5 dataset of buckling values, we now apply various fitting methods [7] (see fig. 9) to fit the buckling values ( $\lambda$ ) as a function of skin thickness ( $t_{skin}$ ) and compression-shear ratio angle ( $\varphi$ ). From various fit assessments, among which a leave-one-out evaluation [7] (see fig. 9), it was concluded that the kriging models and 3<sup>rd</sup> order polynomial (poly3) fits were the most accurate, and because of its computational efficiency the latter was used in the barrel optimization.

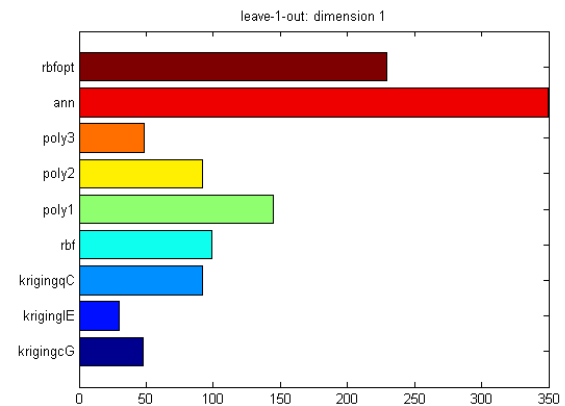


Fig. 9: Results of the fits assessments by leave-one-out evaluation, expressed in root mean squared error (RMSE) value on horizontal axis, of the various fitting methods (indicated in the graph on the vertical axis as poly\* (least squares polynomials), kriging\*\* (kriging models), ann (neural networks) and rbf and rbfopt (radial basis functions)).

The poly3 surrogate model of the panel level buckling values can be directly used in the barrel level optimization. From the local loading condition as obtained from the barrel model (in terms of axial compression and shear load intensities, and expressed by the compression-shear ratio angle), the panel level optimization exists in finding the minimum skin thickness subject to the constraint that the local load intensities in the barrel are lower than the panel buckling load as predicted by the surrogate model.

### 4.3 Barrel level analyses

The barrel level analyses make use of a relatively coarse parametric FEM model, implemented in Abaqus [8], of a cylindrical fuselage barrel with a diameter of about 4300 mm and length of about 11700 mm. Skins are modeled as linear shell elements (S4R [8]), grouped into a ‘crown section’ (barrel skin above the cabin floor) and ‘keel section’ (barrel skin below the cargo floor) for which separate thicknesses can be specified. The barrel model also contains 68 omega stringers (along the full length of the barrel) and 21 C-frames, both with similar shape and pitch as in the panel model, but modeled here by 2-node beam elements (B31 [8]). Also cabin and cargo floors and vertical struts below the cabin floor are included in the barrel model. The floors and struts structures are modeled by flat shell (S4R) elements with 27 (for cabin floor) and 15 (for cargo floor) omega-shaped stringers and 21 C-shaped frames (in both floors and struts), also modeled as B31 elements. The full barrel model contains about 7400 elements (2500 shells (S4R); 4900 beams (B31)), about 2500 nodes and 15000 dofs.

Materials in the barrel model are simplified to isotropic approximations of the materials used in the panel level model:  $E=85\text{GPa}$  and  $\nu=0.35$  for skins,  $E=110\text{GPa}$  and  $\nu=0.35$  for skin-stringers, and aluminium ( $E=72\text{GPa}$ ,  $\nu=0.3$ ) for the frames and all shells, stringers and beams in the floors and struts. All skin-stringers and skin-frames are 2 mm thick, all floors and struts structures are 3 mm thick.

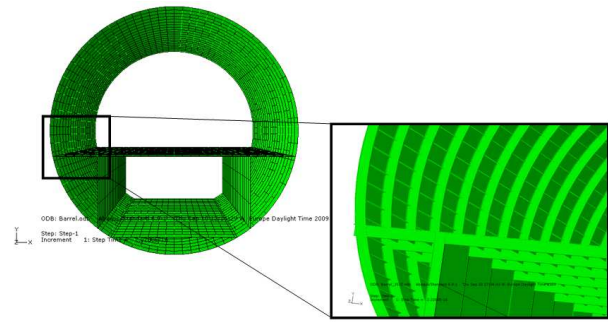


Fig. 10: Illustration of the cylindrical barrel model with skins, stringers, frames, floors and vertical struts structures.

A linear static analysis of the barrel deformation for the considered load-case (see barrel loading in fig. 4 above) is performed, which requires about 15 s CPU time on a standard PC (Pentium 4, 2.8 GHz). The resulting deformation, strains and stresses in the whole barrel structure (see fig. 11 below) resulting from these analyses are then used in the barrel level optimization.

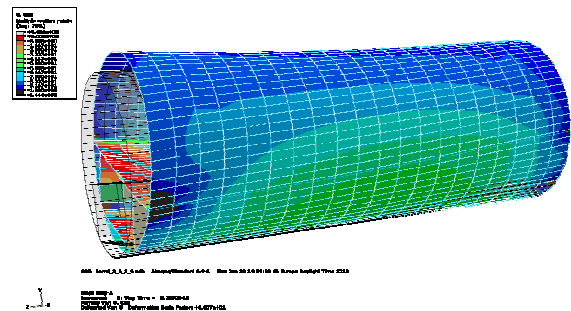


Fig. 11: Illustration of the initial barrel deformation. The colors represent S22 stress values (in fuselage axis direction), indicating higher compressive stress (blue) in the crown region than in the keel region (green).

### 4.4 Main results

In the barrel model we identify two localized regions, in the centers of the crown and keel sections (i.e. the top and bottom skin areas near the mid-frame of the barrel), where we evaluate the local load intensities from the local stresses in the skins, stringers and frames. These load intensities are assumed to be representative for the panel loading in the crown and keel sections, and are used to identify the optimized panel skin thickness from the panel level results. The initial skin thicknesses in the whole barrel are 3mm. The local load intensities

in crown and keel in the initial barrel (table 2. below) yielded the corresponding compression-shear ratio angle ( $\varphi$ ) (table 2. below).

Table 2: Local load intensities in the crown and keel region of the barrel model ( $N_{xx}$  is in barrel axis direction;  $N_{xy}$  is in plane panel shear load intensity;  $N_{yy}$  in circumferential direction was close to zero in the whole barrel for this load-case). The corresponding values of the compression-shear ratio angle  $\varphi$ , computed as  $\varphi = \arctan(N_{xy}/N_{xx})$ , are also given.

	$N_{xx}$ (N/mm)	$N_{xy}$ (N/mm)	$\varphi$	$t_{skin}$ (mm)
Crown-initial	390.4	202.8	27.5	3.0
Keel-initial	211.0	131.6	32.0	3.0
Crown-optimal	384.5	201.3	27.6	2.6
Keel-optimal	171.6	104.9	31.5	1.9

In the barrel level optimization the crown and keel skin thicknesses are minimized, subject to the buckling constraints based on the panel level analyses results. This is achieved by retaining the compression-shear ratio angle ( $\varphi$ ) values in the crown and keel sections, which are computed by  $\varphi = \arctan(N_{xy}/N_{xx})$ . For these  $\varphi$  values the load intensities found in the barrel model are required to be lower than the buckling load predicted by the surrogate model of the panel level buckling values. The optimization iteration exists in updating of the crown and keel skin thicknesses in the barrel model, re-evaluating the local load intensities with the barrel model, and re-evaluating the objective (skin thickness) and constraint function (local load intensities shall be lower than the predicted buckling load) with the surrogate model. This iteration needed 4 steps to converge to an optimal solution for the crown and keel skin thicknesses with an absolute convergence tolerance of 0.1 mm. The resulting values for the optimal crown and keel skin thicknesses are also given in table 2.

## 5 Conclusions and discussion

An implementation of a two-level MLO method has been described. The accuracy and efficiency of this method has been assessed in comparison with a direct (AiO) optimization approach on a test problem based on the 10-bar

truss optimization problem. Furthermore this MLO method has been applied to an optimization of a composite fuselage barrel, in which parametric FEM models of the fuselage barrel and panel were used.

Current results, which are based on relatively simple barrel and panel models, indicate that the described optimization method is feasible and efficient. In only few iterations of the barrel level optimization a feasible optimum was found. We have not compared this result with a direct AiO optimization of the barrel, but it should be noted that for such an AiO optimization the barrel model should be much more detailed in order to be able to predict the local skin buckling constraint that was considered here.

The barrel-panel optimization problem shown here was limited to a simple case, where only one design variable was considered. This was sufficient to demonstrate the applicability of the MLO method to this design case. But a further elaboration of this optimization, e.g. by considering more design variables (like stringer dimensions and composite fiber orientations) and additional constraint functions (e.g. considering local stresses or strains) will allow for more detailed assessment of the benefits of the MLO method. Furthermore, the incorporation of multiple load-cases and more localized regions (representative for local panel loading) in the barrel level analyses would be useful. Work is ongoing to incorporate these aspects in the barrel-panel optimization problem.

The FEM models that are used for the fuselage barrel and panel will need further enhancements, e.g. for the boundary conditions, material behavior and considered load-cases. Because we considered only linear buckling in the panel level analyses, a rather coarse mesh was used here. Still we checked the mesh dependency of the results by applying a double and triple refinement of the mesh in the 2 central bays of the panel, yielding however no significantly different values.

The constraint in the barrel optimization was based on local skin buckling, which was evaluated with the panel level buckling analyses. However, for some of these evaluations, in particular for higher skin thickness and more shear loading, the buckling modes showed an increasing non-local behavior (i.e., modes were not restricted within single bays). Strictly considered these global buckling modes represent a stronger “un-allowable” panel behavior, but because the buckling modes for the optimum values found in the crown and keel were clearly local we accepted this result.

Besides improvements of the barrel and panel models, the development and quality assessment of the surrogate models of the panel can be more extended. For example, only very coarse full-factorial sampling (5x5) of thickness and load ratio was applied here, which could be easily enhanced by applying for example D-optimal or latin-hypercube schemes to improve the sampling efficiency. Moreover, detailed localized (re-)sampling by evaluations of the panel level model (i.e., around the loading found from the barrel analysis) and more advanced surrogate modeling methods like the MoE method that was presented in the 10-bar truss case, was not yet applied in the barrel-panel case. These issues are addressed in ongoing work in this area.

## Acknowledgements

The research leading to these results has received funding from the European Community’s Seventh Framework Programme FP7/2007-2013 under grant agreement n°213371 (MAAXIMUS). The authors thank Ir. F. Grooteman and Ir. M. Nawijn, of NLR, Aerospace Vehicles Division, for their support in the development and evaluation of the panel FEM models.

## References

- [1] Campbell K. Airbus to start manufacturing parts for new A350 XWB in late '09. *Engineering News online*, 11 May 2009.  
<http://www.engineeringnews.co.za/article/airbus-to->

- start-manufacturing-parts-for-new-a350-xwb-in-late-09-2009-05-11 (accessed on 18-08-2009).
- [2] Strong A.B. *Fundamentals of composites manufacturing: materials, methods and applications*. Dearborn, Mich.: Society of Manufacturing Engineers, 2008.
- [3] Balling R.J., Sobieszczanski-Sobieski J. Optimization of Coupled Systems: A Critical Overview of Approaches, AIAA-94-4330-CP, *Proceedings of the 5th AIAA/NASA/USAF/ISSMO Symposium on Multidisciplinary Analysis and Optimization*, pp. 697 - 707, Panama City, Florida, September 7-9 1994.
- [4] Sobieszczanski-Sobieski J., Agte J.S., Sandusky R.R. Bi-level integrated system synthesis, *AIAA/USAF/NASA/ISSMO Symposium on Multidisciplinary Analysis and Optimization*, 7th, St. Louis, MO, Sept. 2-4, 1998, Collection of Technical Papers. Pt. 3 (A98-39701 10-31), AIAA-1998-4916.
- [5] Sobieszczanski-Sobieski J., and Haftka R.T. Multidisciplinary Aerospace Design Optimization: Survey of Recent Developments, AIAA 96-0711, *34th AIAA Aerospace Sciences Meeting and Exhibit*, Reno, Nevada, January 15-18 1996.
- [6] Agte J.S. A Tool for Application of Bi-Level Integrated System Synthesis to Multidisciplinary Design Optimization Problems, DGLR-2005-241, *German Air and Space Congress*, September 2005.
- [7] Vankan W.J., Maas R., Laban M. Fitting fitness in aircraft design, *ICAS 2006 Conference*, September 2006, Hamburg, Germany. NLR-TP-2006-430.
- [8] Abaqus/CAE-6.9-1,  
[http://www.simulia.com/products/abaqus\\_fea.html](http://www.simulia.com/products/abaqus_fea.html)
- [9] Nealen A. An As-Short-As-Possible Introduction to the Least Squares, Weighted Least Squares an Moving Least Squares Methods for Scattered Data Approximation and Interpolation. TU Darmstadt. May 2004.
- [10] Jordan M.I. and Jacobs R.A. Hierarchical mixtures of experts and the EM algorithm. *Neural Computation*, 6, 181-214, 1994.

## Copyright Statement

The authors confirm that they, and/or their company or organization, hold copyright on all of the original material included in this paper. The authors also confirm that they have obtained permission, from the copyright holder of any third party material included in this paper, to publish it as part of their paper. The authors confirm that they give permission, or have obtained permission from the copyright holder of this paper, for the publication and distribution of this paper as part of the ICAS2010 proceedings or as individual off-prints from the proceedings.